Topography of Diphtheria Toxin's T Domain in the Open Channel State

Lisa Senzel,* Michael Gordon,* Robert O. Blaustein,§ K. Joon Oh,‖ R. John Collier,‖ and Alan Finkelstein*‡

From the *Department of Neuroscience and ‡Department of Physiology and Biophysics, Albert Einstein College of Medicine, 1300 Morris Park Avenue, Bronx, New York 10461; §Department of Biochemistry, Brandeis University, Waltham, Massachusetts 02254; ‖Department of Microbiology and Molecular Genetics, Harvard Medical School, Boston, Massachusetts 02115

abstract When diphtheria toxin encounters a low pH environment, the channel-forming T domain undergoes a poorly understood conformational change that allows for both its own membrane insertion and the translocation of the toxin's catalytic domain across the membrane. From the crystallographic structure of the water-soluble form of diphtheria toxin, a "double dagger" model was proposed in which two transmembrane helical hairpins, TH5-7 and TH8-9, anchor the T domain in the membrane. In this paper, we report the topography of the T domain in the open channel state. This topography was derived from experiments in which either a hexahistidine (H6) tag or biotin moiety was attached at residues that were mutated to cysteines. From the sign of the voltage gating induced by the H6 tag and the accessibility of the biotinylated residues to streptavidin added to the cis or trans side of the membrane, we determined which segments of the T domain are on the cis or trans side of the membrane and, consequently, which segments span the membrane. We find that there are three membrane-spanning segments. Two of them are in the channel-forming piece of the T domain, near its carboxy terminal end, and correspond to one of the proposed "daggers," TH8-9. The other membrane-spanning segment roughly corresponds to only TH5 of the TH5-7 dagger, with the rest of that region lying on or near the cis surface. We also find that, in association with channel formation, the amino terminal third of the T domain, a hydrophilic stretch of ~70 residues, is translocated across the membrane to the trans side.

key words: planar bilayers • translocation • histidine tag • streptavidin

INTRODUCTION

Diphtheria toxin is a single, 535-residue polypeptide containing three domains: the amino-terminal C, or catalytic, domain (residues 1–185); the carboxy-terminal R, or receptor-binding, domain (residues 386–535), and the translocation, or T domain, lying between them (residues 202–378) (Fig. 1). The catalytic domain is connected to the T domain by a protease-susceptible loop and by an easily reducible disulfide bridge.

The catalytic domain is an enzyme that catalyzes ADP ribosylation of elongation factor-2 (EF-2), thereby inhibiting protein synthesis and ultimately killing the cell; to gain access to the cytosol where EF-2 resides, it requires the assistance of the other two domains. The toxin first binds via its R domain to a cell surface receptor, and following receptor-mediated endocytosis finds itself in an acidic vesicle compartment. There, through the interaction of the T domain with the endosomal membrane, the catalytic domain is translocated to the cytosol. (For a general review of diphtheria toxin, see Madshus and Stenmark, 1992.) The only apparent function of the endosome in this process is to provide a low pH environment, as it can be experimentally bypassed by briefly pulsing toxin-treated cells to a low pH, in which case the T domain translocates the catalytic domain directly across the plasma membrane (Draper and Simon, 1980; Sandvig and Olsnes, 1980). Under these low pH conditions, whole toxin (and toxin lacking the catalytic domain) also forms channels in the plasma membrane (Eriksen et al., 1994; Lanzrein et al., 1997).

In planar lipid bilayers, the T domain alone, as well as whole toxin and a mutant lacking the R domain, form channels when the pH of the cis side (the solution to which protein is added) is below 6 (Donovan et al., 1981; Kagan et al., 1981). Whatever role these channels may have per se in protein translocation, the entire catalytic domain is translocated across planar lipid bilayers in association with their formation (Oh et al., 1999). Thus, all of the translocation machinery is contained in the T domain; no cellular components, or even the toxin's R domain, are required for translocation. In addition, the amino terminus of the T domain, along with some or all of the adjacent hydrophilic ~70 residues, are also translocated (Senzel et al., 1998). What is the mechanism underlying this prodigious translocation feat of some 270 residues? To begin to address this, we have mapped the T domain's topography in the open channel state. That is, we have determined which parts lie on the cis side, the trans side, and within the membrane.

Lisa Senzel and Michael Gordon contributed equally to this work and should be considered co–first authors.

Address correspondence to Alan Finkelstein, Department of Physiology and Biophysics and Department of Neuroscience, Albert Einstein College of Medicine, 1300 Morris Park Avenue, Bronx, NY 10461. Fax: 718-430-8819; E-mail: finkelst@aecom.yu.edu

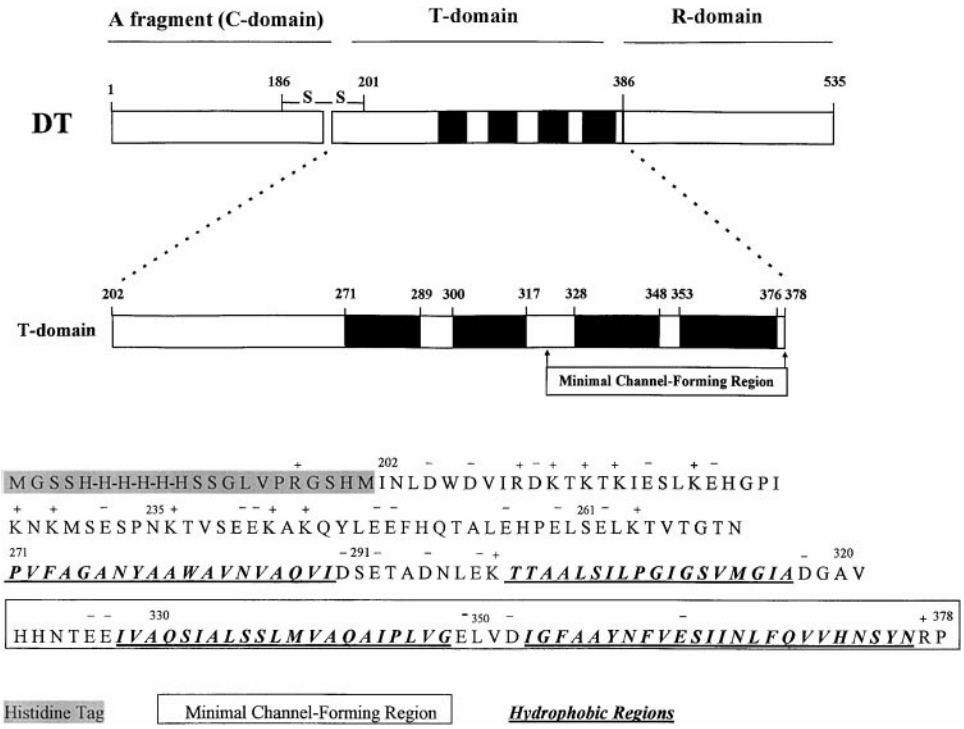

Figure 1. (Top) Linear diagram of the whole diphtheria toxin (DT) molecule (protease nicked), with an expanded view of the channel-forming T domain. Black regions denote hydrophobic stretches within the T domain. (Bottom) Sequence of the H6-tagged T domain, slightly modified from Senzel et al. (1998) and edited to correct two errors in that sequence.

The 177-residue T domain can be subdivided into a very polar amino-terminal third (residues 202–270), with 27 of 69 residues charged, and a carboxy terminal two thirds (271–378) that contains four stretches, each of ~20 residues, with only 2 of 82 residues charged (Fig. 1). The 57 carboxy terminal residues (322–378), which contain two of the nonpolar stretches along with their polar acidic connecting loop, is the minimal channel-forming piece (Silverman et al., 1994a; Huynh et al., 1997); it corresponds to the α-helical hairpin TH8-9 in diphtheria toxin's water soluble form (Choe et al., 1992; Bennett et al., 1994). The other two nonpolar stretches and their polar acidic connecting loop (residues 270–317) correspond to the α-helical hairpin TH5-7 (Choe et al., 1992; Bennett et al., 1994). An obvious possibility is that these two nonpolar α-helical hairpins, seen in the crystal structure of the soluble toxin, are inserted through a membrane like "double daggers," with their acidic connecting loops in the trans solution (Choe et al., 1992). There is considerable evidence from studies on planar bilayers, liposomes, and cells that the segment corresponding to TH8-9 in the crystal structure is so oriented in membranes (see discussion), but there are limited data (discussed later) on the disposition of the segment corresponding to TH5-7. As we shall see, our results on the open channel state confirm the transmembrane orientation of TH8-9, but indicate that only ~TH5 of TH5-7 has a transmembrane orientation. We also establish that the very polar amino terminal third of the T domain is on the trans side of the membrane.

MATERIALS AND METHODS

Mutagenesis and Protein Preparation

The details of site-directed cysteine mutagenesis of the T domain (residues 202–378), which has no natural cysteines, and subsequent protein expression and purification are given by Zhan et al. (1995); the expressed proteins have an amino terminal histidine (H6) tag with the sequence: Gly-Ser-Ser-$(His)_6$-Ser-Ser-Gly-Leu-Val-Pro-Arg-Gly-Ser-His-Met (Senzel et al., 1998). In those experiments in which a synthetic H6 peptide was chemically attached to a cysteine mutant, the amino terminal H6 tag was first removed (except for the experiment in Fig. 12), following manufacturer's instructions (Novagen, Inc.), and confirmed by gel shift assay, leaving four additional amino terminal residues: Gly-Ser-His-Met. (We retain, however, throughout this paper, the numbering system used for native toxin; Greenfield et al., 1983.)

Adding Maleimide Functionality to the Synthetic H6 Peptide

The H6 peptide, Met-Gly-Ser-Ser-$(His)_6$-Ser-Ser-Gly-Leu-Val-Pro-Arg, with the carboxy terminus modified to an amide, was synthesized for us by Chiron Technologies. *N*-hydroxysuccinimidyl 3-maleimidopropionate (SMP) was synthesized by previously published methods (Neilsen and Buchardt, 1991). A maleimidopropionyl group was added to the amino terminus of the H6 peptide via amide bond formation to the free amine by reaction with SMP as follows: 14.4 mg (7.6 μmol) peptide were dissolved in 1 ml of a 20-mM sodium phosphate buffer, pH 7.0, and the resulting acidic solution was titrated to neutrality by addition of 25 μl of 0.1 N NaOH. This solution was added to 1 ml of a 7.6-mM solution of SMP dissolved in acetonitrile, and the resultant solution was stirred for 30 min and centrifuged under vacuum for 10 min to remove the acetonitrile. The desired maleimidopeptide was purified by reverse-phase chromatography using an HPLC system (Waters Corp.) equipped with a semipreparative C18 column (YMC Inc.) and assayed on a Mariner electrospray/TOF mass spectrometer (PE Biosystems/Perkin Elmer). Analysis of the ma-

leimidopeptide on an analytic C18 column demonstrated a purity >95%. Under the above conditions, the yield was ~50%; longer incubations or greater molar excess of SMP did not improve the yield and resulted in extra peaks on HPLC analysis. When assayed by mass spectrometry, these peaks were found to be peptides with more than one maleimide group added, presumably via ester linkage to one or more of the serines present.

Attaching Maleimido-H6 Peptide to T Domain Cysteine Mutants

After removal of the amino terminal H6 tag with thrombin (Novagen, Inc.), single cysteine substitution mutants of T domain at concentrations of 0.2 mg/ml were treated with 20 mM DTT and dialyzed into 150 mM sodium phosphate, 5 mM EDTA, pH 7.0. For each mutant, 30 μl of T domain were mixed with 15 μl of maleimido-H6 peptide (0.8 mg/ml in 100-mM sodium phosphate, pH 7.0). After 3 h at 30°C, the reaction was stopped with 0.5 μl of β-mercaptoethanol. Addition of the maleimido-H6 peptide to the mutants was confirmed by gel shift assay. When wild-type T domain was mixed with maleimido-H6 peptide as a control, no reaction occurred.

Biotinylating T Domain Cysteine Mutants

Biotinylation with *N*-[6-(biotinamido)hexyl]-3′-(2′-pyridyldithio) propionamide (Pierce Chemical Co.) was accomplished as described previously (Qiu et al., 1996). Mutant T267C was also biotinylated with *N*-[2-(biotinamido) ethyl]-3′-(2′-pyridyldithio) propionamide, which has a shorter spacer arm (Qiu et al., 1996). Biotinylation was assessed by an SDS-polyacrylamide gel streptavidin-binding assay (Qiu et al., 1994). Some of the biotinylated mutants were purified using a monomeric avidin column (Pierce Chemical Co.) to remove any residual unbiotinylated protein (Qiu et al., 1996). After elution in PBS/2 mM biotin, fractions were dialyzed into the usual storage buffer (20 mM Tris-Cl, pH 8). Biotinylated mutants purified on monomeric avidin columns showed no evidence of any residual unbiotinylated T domain in the gel assay. In some experiments, biotinylated mutants were premixed with a stoichiometric excess of streptavidin at room temperature for at least 5 min to allow binding, before adding the mixture to the cis solution. Streptavidin was from Calbiochem Corp.

All T domain mutants, including those biotinylated or with attached H6 peptide, were stored frozen at −20° or −80°C at concentrations of 0.2–1.0 mg/ml. Aliquots could be thawed and refrozen numerous times without loss of channel-forming activity.

Bilayer Experiments

Planar lipid (asolectin) bilayer membranes (~100 μm in diameter) were made and recorded from under voltage-clamp conditions as previously described (Senzel et al., 1998). The solutions on both sides of the membrane contained 1 M KCl, 2 mM $CaCl_2$, and 0–1 mM EDTA; in addition, the cis solution (the solution to which T domain was added) contained 5–30 mM Mes, pH 5.3, and the trans solution contained 5–50 mM HEPES, pH 7.2. Voltages are those of the cis solution with respect to the opposite trans solution, whose potential is defined as zero.

RESULTS

Mapping T Domain Topography Using Chemically Attached H6 Peptide

When steps of positive voltage are applied across a membrane with T domain in the cis compartment, the current continuously rises, as channels open (or insert); at negative voltages, these channels close very slowly (Senzel et al., 1998). In contrast, channels formed by T domain having an amino-terminal H6 tag turn off very rapidly at negative voltages; this is because the H6 tag is translocated to the trans side, where it closes the channels (probably by plugging them) (Senzel et al., 1998). We exploited this phenomenon to map T domain topography. We removed the amino-terminal H6 tag from cysteine mutants by proteolytic cleavage, attached a synthetic H6 tag peptide to the cysteine sulfhydryl (see materials and methods), and examined the voltage dependence of the resulting channels. To appreciate the results of these experiments, it is useful to first consider the effect of free synthetic H6 peptide on the voltage gating of T domain channels having no attached H6 tag.

Effect of free synthetic H6 peptide. When free H6 peptide was added to the trans solution to a concentration of 100 μM or more,[1] the T domain–induced conductance decreased rapidly at negative voltages and recovered rapidly at positive voltages (Fig. 2 A). The larger the voltages, the greater the effect. This pattern mimicked that seen with the amino-terminal H6-tagged T domain channels, except that the "block" at negative voltages was less complete (at the free H6 tag concentrations used). At the single channel level, trans free H6 peptide induced rapid channel flickering at negative voltages between the open state and a zero-conductance "blocked state" (Fig. 2 B). At positive voltages, the channel stayed open, apparently unaffected by trans H6 peptide. With H6 peptide in the cis solution, voltage gating, both macroscopic and single-channel, was essentially the same as with H6 peptide in the trans solution, except the sign was reversed. That is, rapid blocking occurred at positive voltages and rapid unblocking at negative voltages (Fig. 3). These results are consistent with a voltage-dependent blockade of the channel by the positively charged H6 peptide.

Effect of H6 peptide attached to residues 235, 261, or 267. When the synthetic H6 peptide was tethered to residues 235, 261, or 267 of T domain lacking an amino terminal H6 tag, the T domain–induced conductance declined rapidly at negative voltages and recovered rapidly at positive voltages (Fig. 4 A). The behavior resembled that seen previously when the H6 tag was at the amino terminus (Senzel et al., 1998), except that larger negative voltages were required in the present instances to obtain comparable effects. As in that case, addition of micromolar quantities of nickel (which complexes histidines) to the trans solution inhibited

[1]An impure preparation of synthetic H6 peptide was used in these experiments. Subsequent HPLC fractionation revealed that peptide containing the NH_2-terminal chemical blocking agent fluorenylmethoxycarbonyl was much more effective than peptide with a free NH_2-terminal amine. Thus, the concentration of effective agent in this section's experiments was considerably less than the nominal concentration.

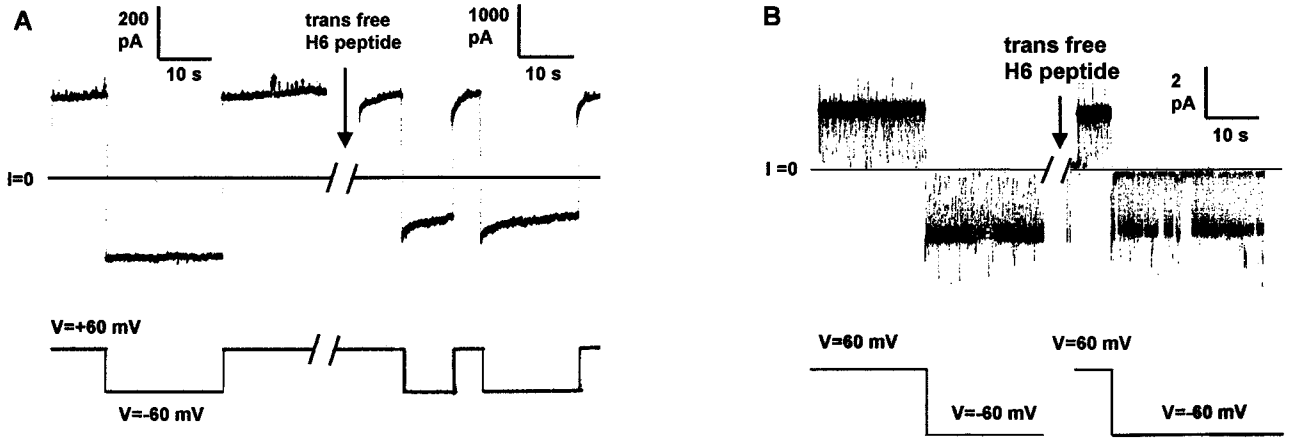

Figure 2. Free H6 peptide, added to the trans side, blocks T domain channel conductance at negative voltages. Before the start of each record, T domain lacking an amino terminal H6 tag was added to the cis compartment to a concentration of ~200 (A) or 1 (B) ng/ml. (A) T domain–induced conductance is seen rising at +60 mV; when the voltage was switched to −60 mV, the conductance remained on. When the voltage was switched back to +60 mV, it continued to slowly rise. Approximately 7 min into the ~15-min break, free H6 peptide was added to the trans solution to a concentration of 200 μg/ml; during the break, T domain–induced conductance continued to rise, reflecting the continual insertion of channels in the membrane. In the presence of trans H6 peptide, conductance turned off rapidly, but incompletely, at −60 mV. When the voltage was switched back to +60 mV, conductance rapidly recovered. (B) In the absence of H6 peptide, a single T domain channel stayed open at +60 and −60 mV, with unresolvably brief flickers to a zero-conductance closed state. During the 4-min break, free H6 peptide was added to the trans solution to a concentration of 100 μg/ml. In the presence of trans H6 peptide, the channel, at +60 mV, behaved the same as before H6 addition; at −60 mV, it flickered rapidly between the open state and a prolonged zero-conductance blocked state. The solutions on both sides of the membrane were 1 M KCl, 2 mM $CaCl_2$; the cis solution contained 30 mM Mes, pH 5.3, and the trans contained 50 mM HEPES, pH 7.2. The records were filtered at 100 Hz by the chart recorder.

the H6 tag effect, and trans EDTA (which chelates nickel) reversed the nickel effect (Fig. 4 A).

At the single channel level, channels flickered rapidly at modest negative voltages between the open state and a zero-conductance blocked state (Fig. 4 B), and were completely blocked at larger negative voltages (−80 mV). When the sign of the voltage was reversed, the channel recovered immediately to the open state. After addition of nickel to the trans solution, the channel spent more time in the open state at negative voltages, and trans

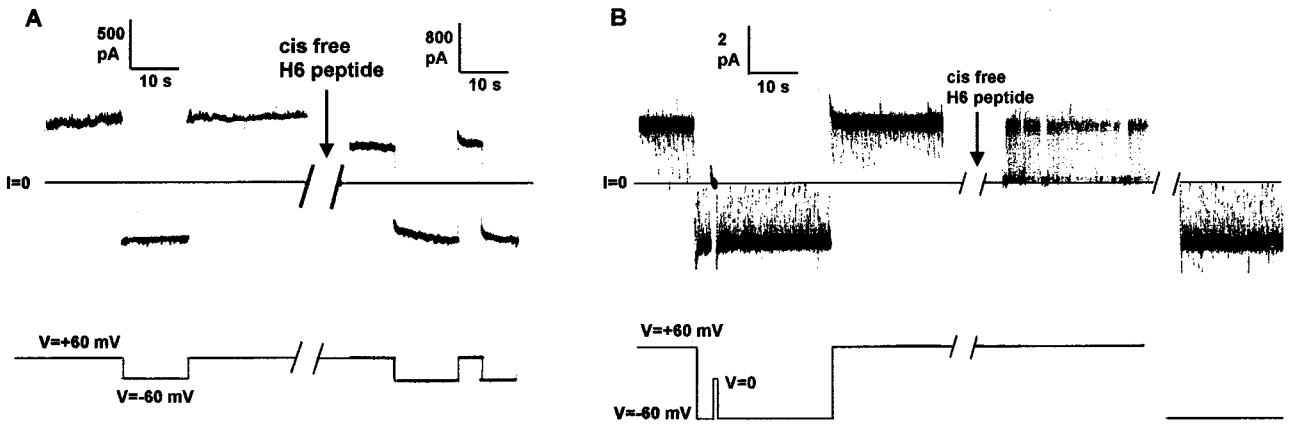

Figure 3. Free H6 peptide, added to the cis side, blocks T domain channel conductance at positive voltages. Before the start of each record, T domain lacking an amino terminal H6 tag was added to the cis compartment to a concentration of ~30 (A) or 0.1 (B) ng/ml. (A) T domain–induced conductance before addition of H6 peptide resembled that seen in Fig. 2 A. Approximately 3 min into the ~23-min break, free H6 peptide was added to the cis solution to a concentration of 100 μg/ml; during the break, T domain–induced conductance continued to rise, reflecting the continual insertion of channels. In the presence of cis H6 peptide, conductance was reduced at +60 mV, compared with that at −60 mV. When the voltage was switched to −60 mV, conductance recovered rapidly; when it was switched back to +60 mV, conductance rapidly decreased. (B) In the absence of H6 peptide, a single T domain channel stayed open at +60 and −60 mV, with unresolvably brief flickers to a zero-conductance closed state. During the 1.5-min break, free H6 peptide was added to the cis solution to a concentration of 100 μg/ml. In the presence of cis H6 peptide, when the voltage was held at +60 mV, the channel flickered rapidly between the open state and a prolonged zero-conductance blocked state. When the voltage was switched to −60 mV after a 1-min break, the channel behaved the same as before H6 peptide addition. Solutions and filtering were as given in Fig. 2.

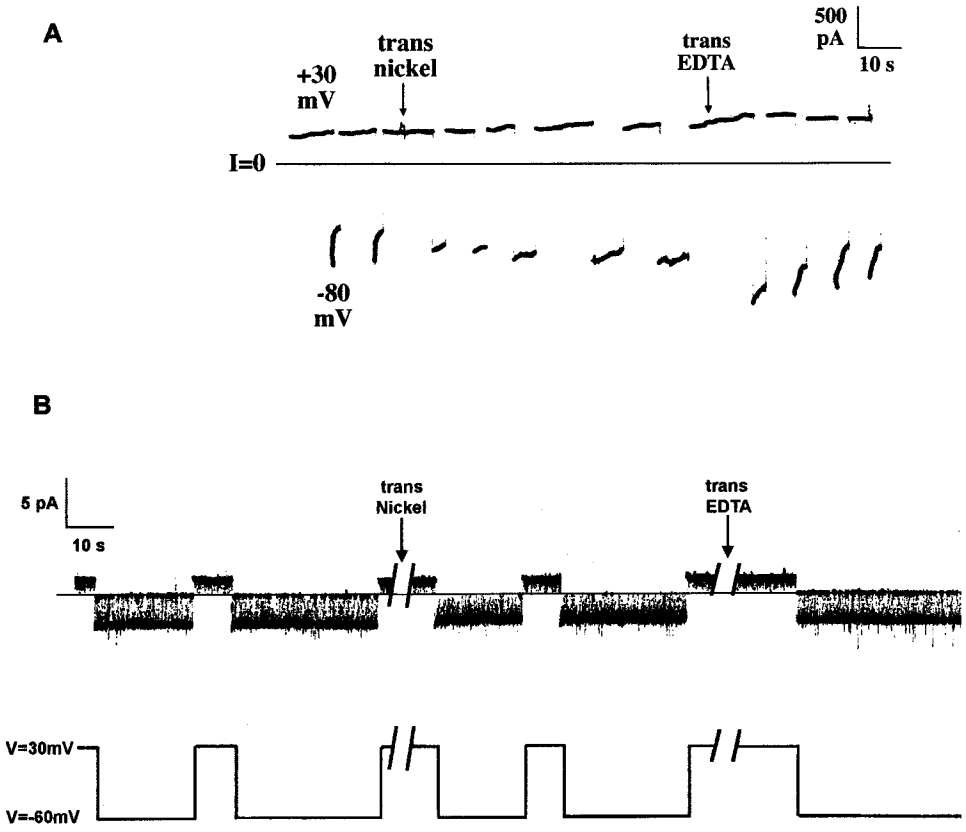

Figure 4. H6 peptide chemically linked at residue 235 blocks the T domain channel at negative voltages; trans nickel inhibits this block. Before the start of each record, T domain with H6 peptide attached at residue 235 was added to the cis compartment to a concentration of ~240 (A) or 480 (B) ng/ml. (A) T domain–induced conductance is seen rising at +30 mV; when the voltage was switched to −80 mV, the conductance decreased rapidly. When the voltage was switched back to +30 mV, the conductance recovered immediately. At the first arrow, $NiSO_4$ was added to the trans solution to a concentration of 25 μM. Subsequently, when the voltage was switched to −80 mV, the conductance turned off very slowly. At the second arrow, EDTA was added to the trans solution to a concentration of 1.8 mM. When the voltage was switched to −80 mV, the conductance again decreased rapidly. (B) A single T domain channel stayed open at +30 mV, with unresolvably brief flickers to a zero-conductance closed state, but flickered between the open state and a prolonged zero-conductance blocked state at −60 mV. During the 15-s break, $NiSO_4$ was added to the trans solution to a concentration of 80 μM. Subsequently, the channel was "unblocked" at −60 mV. During the 2-min break, EDTA was added to the trans solution to a concentration of 2.4 mM, and the channel then resumed flickering to a zero-conductance blocked state at −60 mV. (Records similar to those in A and B were obtained with T domain having the H6 peptide attached at residue 261 and 267.) The solutions on both sides of the membrane were 1 M KCl, 2 mM $CaCl_2$; the cis solution contained 8 mM Mes, pH 5.3, 1 mM EDTA, and the trans solution contained 50 mM HEPES, pH 7.2, and 5 μM EDTA. The records were filtered at 10 (A) or 100 (B) Hz by the chart recorder.

EDTA reversed the nickel effect (Fig. 4 B). Thus, macroscopic and single-channel data were in agreement.

The voltage gating of channels formed by T domain with an H6 tag at the amino terminus results from the H6 tag being translocated to the trans solution (Senzel et al., 1998). The same conclusion, by analogy, can be drawn in the present case. This is confirmed, moreover, by our findings that the H6 tag at residue 235, 261, or 267 interacts with trans Ni^{2+} (Fig. 4) and that the sign of the voltage gating is the same as that induced by direct addition of free synthetic H6 peptide to the trans solution (Fig. 2). Thus, in association with channel opening, not only is the amino terminus of the T domain translocated (Senzel et al., 1998), but so are residues 235, 261, and 267. We can therefore reasonably conclude that the entire very polar amino-terminal third (residues 202–270) of the T domain is translocated to the trans side.

Effect of H6 peptide attached to residues 291, 293, 294, 320, or 376. When the synthetic H6 peptide was tethered to either residue 291, 293, 294, 320, or 376, the T domain conductance declined very rapidly at positive voltages and increased very rapidly at negative voltages (Fig. 5 A). (The transients were too fast to be recorded at our 100-Hz filtering.) At the single-channel level, the channels spent most of their time in a zero-conductance blocked state at +60 or +80 mV; when the sign of the voltage was reversed, the channels recovered immediately to the open state (Fig. 5 B). Thus, at both the macroscopic and single-channel levels, channels with tethered H6 peptide at these residues qualitatively displayed the same voltage-dependent behavior as that induced by free H6 peptide added to the cis solution, thereby demonstrating that these residues remain on the cis side when T domain channels open. As expected, trans nickel had no effect on the gating of these channels.[2]

Mapping T Domain Topography Using The Biotinylation–Streptavidin Assay

As a second method for determining a residue's location, we examined the effect of streptavidin on channels

[2]Cis nickel was also without effect, but this is not surprising, since at the cis pH (5.3), Ni^{2+} complexes poorly with histidines.

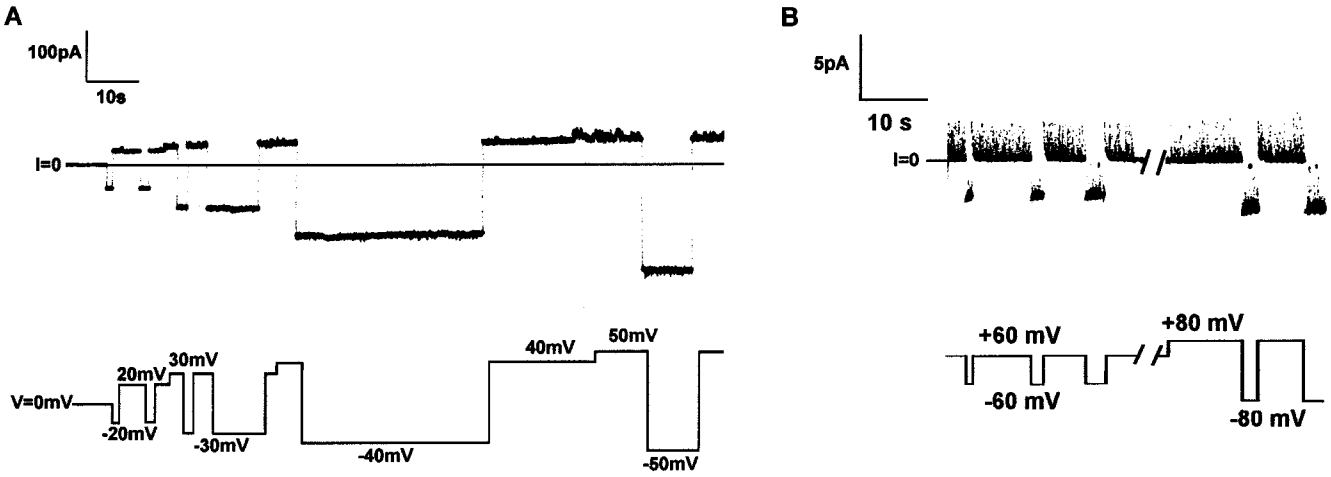

Figure 5. H6 peptide chemically linked at residues 293 or 320 blocks the T domain channel at positive voltages. Before the start of each record, T domain with H6 peptide attached at residue 293 (A) or 320 (B) was added to the cis compartment to a concentration of ~300 (A) or 400 (B) ng/ml. (A) After addition of the T domain, conductance rose over time to the level seen at the start of the record, with the voltage held at +20 mV. When the voltage was switched to −20 mV, the conductance nearly doubled. Subsequent voltage steps to +30, +40, and +50 mV with intervening pulses to corresponding negative voltages demonstrated two facts. (a) The conductance at each positive test voltage was less than that at the corresponding negative voltage; the magnitude of the rectification increased with larger voltages. (b) Positive 10-mV increments produced disproportionately small current increases. (B) A single channel flickered between the open state and a zero-conductance blocked state at +60 mV, spending almost all its time in the zero-conductance state. When the voltage was switched to −60 mV, the channel became unblocked. Similar behavior was seen at ±80 mV after a 1-min break. (Records similar to those in A and B were obtained with T domain having the H6 peptide attached at residue 376, 291, or 294.) The solutions on both sides of the membrane contained 1 M KCl, 2 mM $CaCl_2$, 1 mM EDTA; the cis solution contained 30 mM Mes, pH 5.3, and the trans contained 50 mM HEPES, pH 7.2. The records were filtered at 100 Hz by the chart recorder.

formed by biotinylated cysteine mutants (see materials and methods). (The biotinylated mutants also contained the amino terminal H6 tag.) If a biotinylated residue is located on either the cis or trans side of the membrane in the channel's open state, streptavidin addition to the appropriate solution could affect channel behavior. Furthermore, pre-exposure to streptavidin of biotinylated residues normally translocated to the trans side in association with channel opening should interfere with channel formation by preventing the translocation. The biotinylation–streptavidin assay was originally employed to map the topography of the colicin Ia channel (Qiu et al., 1996), and was recently used to demonstrate that diphtheria toxin's catalytic domain is translocated across planar lipid bilayers (Oh et al., 1999).

Residues 235, 261, and 267. In the previous section, we showed, with chemically attached H6 peptide, that these residues were on the trans side of the membrane. The biotinylation–streptavidin assay confirmed this. Trans streptavidin produced a small increase in the conductance induced by these biotinylated mutants, and a large increase in current noise (Fig. 6); both effects were reversed by addition to the trans side of the membrane-impermeant disulfide reducing agent TCEP [tris(2-carboxy-ethyl)phosphine] (Fig. 6), which can reduce the disulfide bond linking biotin to the cysteine residue, thereby removing biotin along with its bound streptavidin. Cis streptavidin had no effect on conductance and noise. The above trans streptavidin effects were not seen if free biotin was added to the trans solution before streptavidin addition, thereby confirming that the effects resulted from streptavidin's binding to the cysteine-attached biotin moiety. In control experiments, trans streptavidin had no effect on wild-type or unbiotinylated mutant channels. The binding of trans streptavidin to biotinylated mutants 235, 261, and 267 had no discernible effect on channel gating by the T domain's amino terminal H6 tag, in contrast to the binding of trans streptavidin to biotinylated mutants 58 and 146, which inhibited channel gating by whole toxin's amino terminal H6 tag (Oh et al., 1999).

If residues 235, 261, and 267 are translocated to the trans side in association with channel formation, preincubating the biotinylated mutants with streptavidin should interfere with channel formation. Such was indeed the case for the biotinylated 235 mutant. (Because of poor expression of the S261C and T267C mutants, we could not purify their biotinylated products on our avidin column, and therefore preincubation results were confounded by channel formation by contaminating residual unbiotinylated molecules.) When biotinylated mutant 235 was preincubated with streptavidin, and then added to the cis solution, typically there was no (or a small, very noisy) induced conductance, or the membrane broke. Thus, as expected, holding residue 235 on the cis side with streptavidin prevented nor-

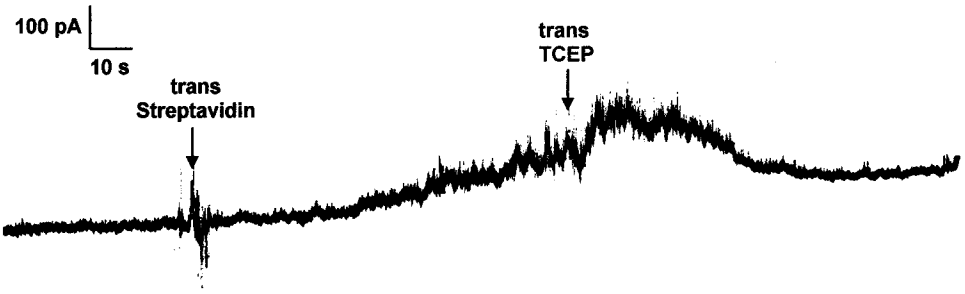

Figure 6. Trans streptavidin reversibly increases the conductance and noise induced by T domain channels biotinylated at residue 261. Before the start of the record, T domain biotinylated at residue 261 was added to the cis compartment to a concentration of ~200 ng/ml. During the entire time, the voltage was held at +30 mV. Conductance increased linearly for several minutes, to ~3.7 nS (~90 channels) at the start of the record. At the first arrow, streptavidin was added to the trans solution to a concentration of 25 μg/ml. Subsequently, both the conductance and the noise increased significantly. At the second arrow, TCEP was added to the trans solution to a concentration of 20 mM, to remove the biotin with its attached streptavidin. After a transient increase in noise (caused by stirring) and conductance, the noise decreased to prestreptavidin levels, and the conductance returned to the pattern of linear rise seen before streptavidin addition. (Similar records were obtained with the biotinylated 235 mutant.) Solutions and filtering were as given in Fig. 5.

mal channel formation. (Occasionally, after a delay, there occurred a rapid incorporation of hundreds of channels into the membrane. The resulting large conductance displayed the normal voltage gating produced by the amino-terminal H6 tag, indicating that it was translocated across the membrane despite residue 235 being bound to streptavidin. A possible explanation of this is considered in the discussion.)

Residues 291, 293, 294, 320, and 376. In an earlier section, we showed, with chemically attached H6 peptide, that these residues remained on the cis side of the membrane. The biotinylation–streptavidin assay confirmed this for residues 291 and 376. The effect of cis streptavidin on the conductance induced by these biotinylated mutants was essentially the same as that produced by trans streptavidin on the biotinylated 235, 261, and 267 mutants (Fig. 7). Trans streptavidin had no effect on conductance and current noise, and earlier cis free biotin addition prevented the effect of subsequent cis streptavidin addition. In control experiments, cis streptavidin had no effect on wild-type or unbiotinylated mutant 291 and 376 channels. Cis streptavidin's effect on current noise resulted from its binding to pre-existing channels and not from streptavidin-bound molecules in solution inserting into the membrane to form new channels. We know this since the pH of the cis solution was raised to 7.2 in most experiments before streptavidin addition, and, at this pH, new channels are not formed (Kagan et al., 1981). Cis TCEP reversed streptavidin's effect on the conductance induced by biotinylated 376 mutant, but not by biotinylated 291 mutant. Cis streptavidin had no discernible effect on biotinylated 320 mutant channels. Biotinylated 293 and 294 mutants did not induce normal channel-forming activity. Although the currents resulting from positive voltage stimuli initially evolved normally, they subsequently became very noisy and ragged, and remained so at negative voltages.

Single channel results. The cis and trans streptavidin-induced increases in macroscopic current noise described above were not reflected in an increase in single-channel current noise, but were seen with as few as 12 channels present (Fig. 8). At this level, it was apparent that streptavidin induced current flickerings to larger, but not to smaller, values (Fig. 8). Thus, streptavidin's effect on current noise does not result from its transiently blocking channels, in which case increased flickering closures should have occurred. Whatever the mechanism, the streptavidin assay clearly locates residues 235, 261, and 267 on the trans side and residues 291 and 376 on the cis side, in agreement with the findings from the chemically attached H6 peptide assay.

Residues 347, 348, and 351. The minimal T domain piece required to form a normal channel is the 57-residue carboxy terminal segment (residues 322–378) (Silverman et al., 1994a; Huynh et al., 1997) that roughly corresponds to the α-helical hairpin TH8-9 (Choe et al., 1992; Bennett et al., 1994). Except for residue 376, lying near the carboxy terminus of this segment, the residues mapped in the previous sections lie outside the actual

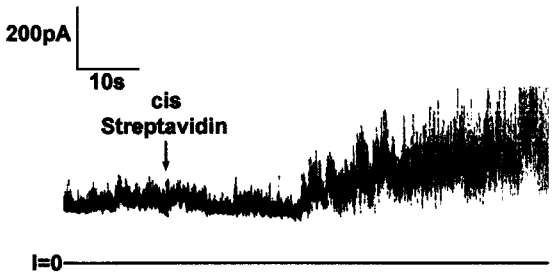

Figure 7. Cis streptavidin increases the conductance and noise induced by T domain channels biotinylated at residue 291. Before the start of the record, T domain biotinylated at residue 291 was added to the cis compartment to a concentration of ~100 ng/ml. Channel conductance increased for several minutes. Approximately 2.5 min before the start of the record, HEPES was added to the cis solution (final concentration 70 mM) to bring the cis pH to ~6.8. During the entire record, the voltage was held at +60 mV. At the arrow, streptavidin was added to the cis compartment to a concentration of 25 μg/ml. Subsequently, both the conductance and the noise increased. (Similar records were obtained with the biotinylated 376 mutant.) Solutions and filtering were as given in Fig. 5.

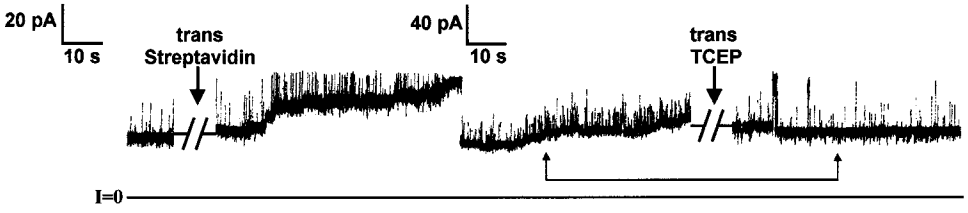

Figure 8. The nature of the streptavidin-induced noise. Before the start of the record, T domain biotinylated at residue 261 was added to the cis compartment to a concentration of ~50 ng/ml. During the entire experiment, the voltage was held at +60 mV, except for occasional pulses to 0 mV during the breaks. Conductance increased linearly for several minutes. Before the first arrow, it was 467 pS, corresponding to ~12 channels. At the first arrow (during a 25-s break), streptavidin was added to the trans compartment to a concentration of 30 μg/ml. Immediately after streptavidin addition, the amount of noise increased significantly, and the conductance increased slowly to ~1.4 nS, corresponding to 35 channels. Note that the noise represents fluctuations to higher, not lower, conductances. During the second break, lasting 4.5 min, conductance continued to rise slowly, to a level of 1.5 nS, corresponding to ~37 channels. TCEP, pH 7.1, was then added to the trans compartment to a concentration of 20 mM. Subsequently, the conductance fell to the level seen after the break, and the noise decreased drastically. The connected arrows show points in the record of equal conductance (~32 channels) before and after TCEP addition; note the difference in noise at these points. The solutions on both sides of the membrane contained 1 M KCl, 2 mM $CaCl_2$, 1 mM EDTA; the cis solution contained 5 mM Mes, pH 5.3, and the trans contained 5 mM HEPES, pH 7.2. The records were filtered at 100 Hz by the chart recorder.

channel. Previous mapping of the channel itself indicated that residues near 348 are close to the trans side of the membrane (Huynh et al., 1997). We sought to independently confirm this placement by the methods described here for mapping residues outside the channel. We were unsuccessful in doing this with the chemically attached synthetic H6 peptide assay since, when it was tethered to either residue 347 or 351, the resulting channels did not display H6 tag gating (see discussion). That is, the attached H6 tag did not block channels at either negative or positive voltages. However, we were successful with the biotinylation–streptavidin assay.

For the biotinylated 347 mutant, trans streptavidin reproducibly caused a fourfold decrease in macroscopic conductance, which was reversed by trans TCEP (Fig. 9 A). In control experiments, cis TCEP did not reverse the trans streptavidin effect, whereas subsequent trans TCEP did. (Because TCEP can cross the membrane at pH 5.3, the control experiments were done at symmetric pH 6.2.) With several channels inserted in the membrane, trans streptavidin caused closure of most channels, and subsequent trans TCEP addition reopened them (Fig. 9 B). [Trans TCEP alone (without earlier streptavidin addition) had no apparent effect on macroscopic conductance, but did increase single channel size slightly, from ~23 to ~30 pS.] Thus, residue 347 is exposed to the trans solution.

As expected, if this residue is translocated across the membrane to the trans side, addition of biotinylated 347 mutant to a streptavidin-containing cis solution produced little or no conductance. If free biotin was then added to occupy all available streptavidin sites, subsequent addition of more biotinylated 347 mutant produced a normal level of conductance. This provided an internal control for the lack of activity observed for the biotinylated mutant exposed to streptavidin earlier in the experiment.

In response to positive voltage steps, the biotinylated 351 mutant produced very noisy and ragged currents, which remained so in response to subsequent negative voltage steps. Thus, biotinylation at this site disrupted normal channel formation. The biotinylated 348 mutant induced currents that looked normal at positive voltages, but noisy at negative voltages. Consistent with residues 348 and 351 being normally translocated across the membrane, addition to the cis solution of biotinylated mutants 348 and 351 preincubated with streptavidin resulted in little or no conductance. (Occasionally, the 351 mutant caused a burst in activity that broke the membrane.)

Huynh et al. (1997) reported that biotinylated 350 or 351 mutants preincubated with streptavidin induced normal channel behavior. It turned out, however, that these mutants were only ~90% biotinylated. Once we separated the biotinylated 351 mutant from unbiotinylated mutant on a monomeric avidin column, the results reported in the previous paragraph were obtained. Thus, in the experiments of Huynh et al. (1997), the 10% of unbiotinylated 351 mutant actually caused the observed channel activity, which was of course unaffected by preincubation with streptavidin. The same was presumably the case in their experiments with the 350 mutant.

DISCUSSION

The interaction at low pH (≤6) of the 177-residue T domain (residues 202–378) of diphtheria toxin with endosomal or plasma membranes results in translocation of the toxin's catalytic domain (residues 1–185) across the target membrane into the cytosol. Under these same low pH conditions, the T domain also forms channels in planar lipid bilayers (and plasma membranes). In association with this channel formation, the catalytic domain is also translocated across planar bilayers (Oh et al., 1999), although the channel's role, if any, in this process is unclear. Thus, the T domain contains the entire translocation machinery; no other proteins, or even the receptor-

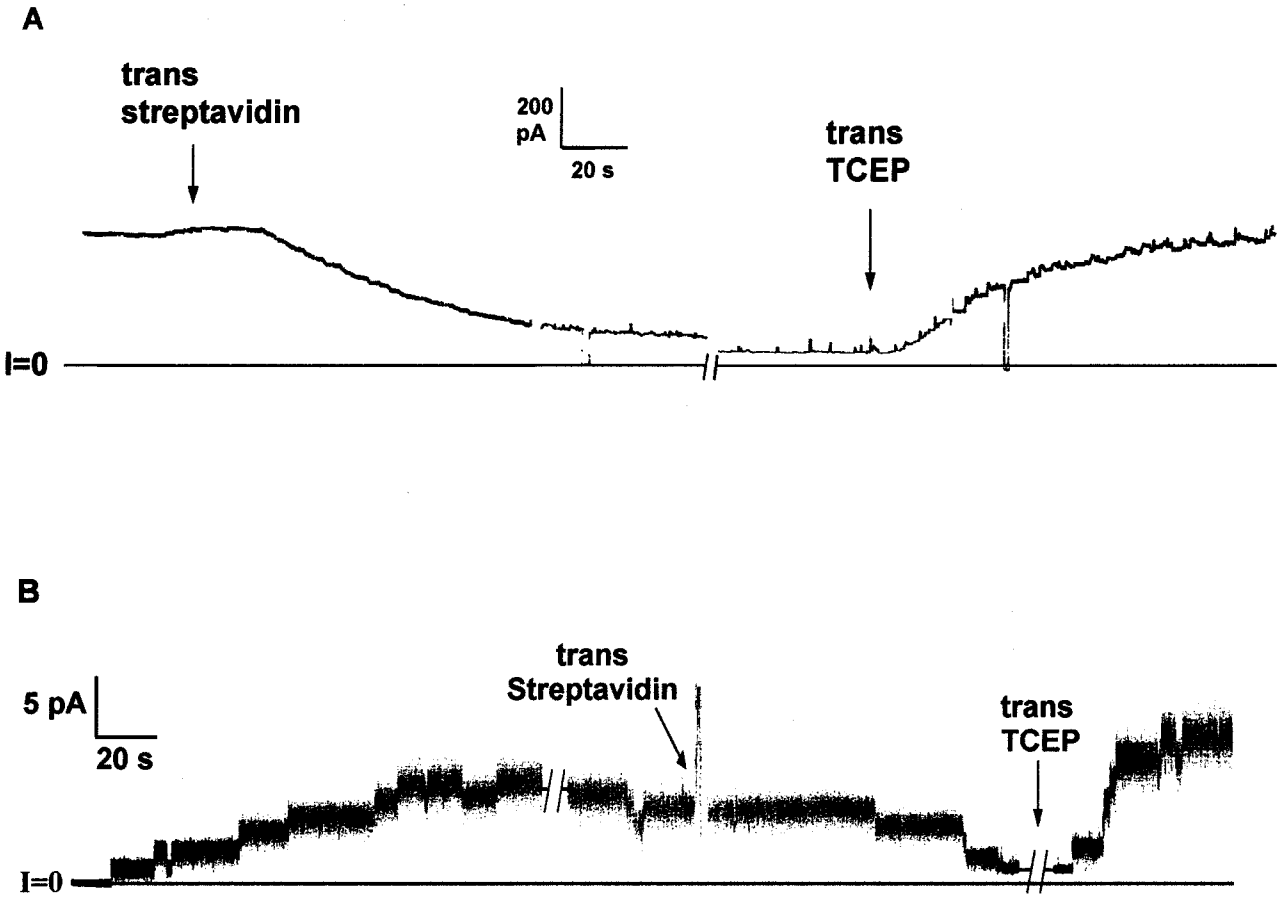

Figure 9. Trans streptavidin reversibly affects conductance induced by T domain channels biotinylated at residue 347. Before the start of each record, T domain biotinylated at residue 347 was added to the cis compartment to a concentration of ~400 (A) or 10 (B) ng/ml. (A) Macroscopic record. Conductance increased for several minutes to the level seen at the beginning of the record. (During the entire experiment, the voltage was held at +40 mV, except for occasional pulses to 0 mV.) At the first arrow, streptavidin was added to the trans solution to a concentration of 25 μg/ml. Over the next 2 min, conductance decreased fourfold. During the 9-min break, the pHs of the cis and trans solutions were brought to 6.2 with Mes (final concentrations 45 mM cis, 25 mM trans), compounding the streptavidin-induced decrease in conductance. At the second arrow, TCEP, pH 6.2, was added to the trans solution to a concentration of 50 mM. Over the next 1.5 min, conductance rose back to prestreptavidin levels. (B) Several channels record. Channels inserted for several minutes, to a level of about six channels. (The voltage was held at +60 mV, except for occasional brief pulses to 0 and −60 mV during the breaks.) Before the first break, streptavidin was added to the cis compartment to a concentration of 30 μg/ml to prevent further incorporation of new channels in the membrane. During the first (1.2-min) break, streptavidin was added to the trans compartment to a concentration of 12 μg/ml, without stirring, and one channel closed. At the first arrow, streptavidin was added (with stirring) to the trans compartment to a final concentration of 25 μg/ml. Subsequently, channels closed to the level of a single open channel. During the second (2-min) break, TCEP was added to the trans compartment to a concentration of 47 mM, and immediately channels rapidly opened until the number exceeded the prestreptavidin level, and then reached a steady state. The solutions on both sides of the membrane contained 1 M KCl, 2 mM $CaCl_2$, 1 mM EDTA; the cis solution contained 5(A) and 30 (B) mM Mes , pH 5.3; the trans contained 5 A) and 50 (B) mM HEPES, pH 7.2. The records were filtered at 10 (A) or 100 (B) Hz by the chart recorder.

binding portion of the toxin (residues 386–535), are required for translocation. How does the T domain accomplish this? This paper begins to address this question by outlining the T domain's topography in the channel's open state. That is, we have determined which of its regions lie on the cis and trans sides of the membrane, and which, by inference, reside within the membrane.

We used two strategies to map the topography. Both of them used substituted cysteine mutagenesis, followed by linking prosthetic groups at the selected sites. In the first, we chemically linked a synthetic hexahistidine (H6) tag to each site. In so doing, we exploited the phenomenon of a voltage-dependent channel block by the H6 tag.[3] Added to the cis solution, the free synthetic H6 peptide blocks channel conductance at positive voltages; added to the trans solution, it blocks

[3]Although the mechanism by which the H6 tag closes T domain channels is not definitely established, it most likely is acting as a channel blocker.

at negative voltages. Hence, if the chemically attached H6 tag blocked the channel at positive voltages, this constituted evidence that the H6 tag, and the residue to which it was linked, was located on the cis side; channel block at negative voltages suggested the opposite location. Interference of H6 tag channel block by micromolar concentrations of trans nickel further confirmed a residue's trans location.

In the second approach, we employed a biotinylation–streptavidin assay. Its rationale was that if a biotinylated residue is located on either the cis or trans side, streptavidin addition to the appropriate solution would likely affect some aspect of channel behavior. We found that streptavidin binding after channel formation generally resulted in an increase in current magnitude and noise; for residue 347, it resulted in channel closure. Furthermore, if a residue ultimately resides on the trans side, its binding to streptavidin before membrane insertion should interfere with channel formation by preventing it from reaching the trans side, which was indeed what we found. The results of both approaches lead us to propose the model for T domain topography shown in Fig. 10, which we now proceed to explicate.

Evidence for the Model

Both the H6 tag and the biotinylation–streptavidin assay place residues 235, 261, and 267 on the trans side of the membrane (Figs. 4 and 6); the inhibition of normal channel formation by preincubating biotinylated 235 mutant with streptavidin supports this conclusion. Given that the T domain's amino terminus is also translocated to the trans solution (Senzel et al., 1998), we conclude that the entire very polar amino-terminal third of the T domain (residues 202–270) is translocated across the membrane to the trans side. In fact, since the catalytic domain of whole toxin is also translocated (Oh et al., 1999), all of the toxin's first 270 residues move across the membrane in association with channel formation!

The H6 assay places residues 291, 293, and 294 on the cis side (Figs. 5 and 7), implying that the polar 10-residue acidic segment, residues 290–299 (Fig. 1), lies there. (The biotinylation–streptavidin assay confirmed this for residue 291; see the next section for residues 293 and 294.) Connecting the dots, this means that the hydrophobic segment consisting of residues 271–289 traverses the membrane. This segment is slightly longer than the TH5 helix seen in the crystal structure of the water soluble form of the toxin (Choe et al., 1992; Bennett et al., 1994). It is tempting to suppose that this hydrophobic segment remains α-helical in the membrane-associated form of the T domain, as it is long enough to traverse the bilayer.

The H6 tag assay places residue 320 on the cis side (Fig. 5), implying that the charged 10-residue segment, residues 318–327 (Fig. 1), lies there. Between the two charged segments (residues 290–299 and 318–327) on the cis side of the membrane is an 18-residue uncharged segment (residues 300–317) corresponding to helices TH6 and TH7 (essentially one helix, TH6-7) in the crystal structure (Choe et al., 1992; Bennett et al., 1994). A helical wheel representation of TH6-7 depicts it as amphipathic. We suggest that this segment retains its helical character, with its nonpolar surface dipping into the hydrophobic portion of the bilayer's cis leaflet, while its polar surface contacts this leaflet's headgroups and the nearby water layer. We have no direct experimental evidence to support this suggestion, but it is the most parsimonious model consistent with its connecting two charged segments lying on the cis surface.

It is interesting to compare the topography presented so far with that inferred from the crystal structure of the toxin's water soluble form; in particular, the portion from TH5 to TH6-7. In the crystal structure, this forms an α-helical hairpin. The obvious inference is that this inserts as such into the membrane, with its acidic connecting loop (residues 290–299) facing the trans solution, and with the amino terminus of TH5 (residue 274) and the carboxy terminus of TH6-7 (residue 315) close to the cis surface (Fig. 11). Our data directly contradict this disposition of the TH5 to TH6-7 region. The acidic connecting loop (residues 290–299) cannot be facing the trans solution, since residues 291, 293, and 294 face the cis solution. (Similarly, our placement of residue 267 on the trans side makes it unlikely that residue 274 is close to the cis surface.) Our results are consistent with only TH5 (not both TH5 and TH6-7) spanning the membrane (Fig. 10), with an orientation opposite that in the double dagger model (Fig. 11).

We turn now to the carboxy terminal end (residues 322–378), which actually forms the channel (Silverman et al., 1994a; Huynh et al., 1997). In the crystal structure, most of this region (residues 318–376) forms the α-helical hairpin TH8-9 (Choe et al., 1992; Bennett et al., 1994). In planar bilayers, pH mutagenesis–titration experiments (Mindell et al., 1994a,b), as well as studies of accessibility of cysteine mutants to sulfhydryl-specific reagents (Huynh et al., 1997), clearly place residues 326–336 closer to the cis than to the trans side, and residues 348–352 close to the trans side. Our experiments placing residue 320 on the cis side (Fig. 5) and residue 347 on the trans side (Fig. 9) confirm these earlier findings that most of helix TH8 spans the membrane (though not necessarily as an α-helix; Huynh et al., 1997). The disposition of helix TH9 is less clear, but residue 359 appears not as close to the trans side as residue 351 (Huynh et al., 1997). Combining this fact with our present finding (by both assays) that residue 376 is on the cis side (Figs. 5 and 7) justifies our having TH9 span the membrane (Fig. 10), although not necessarily as an α-helix.

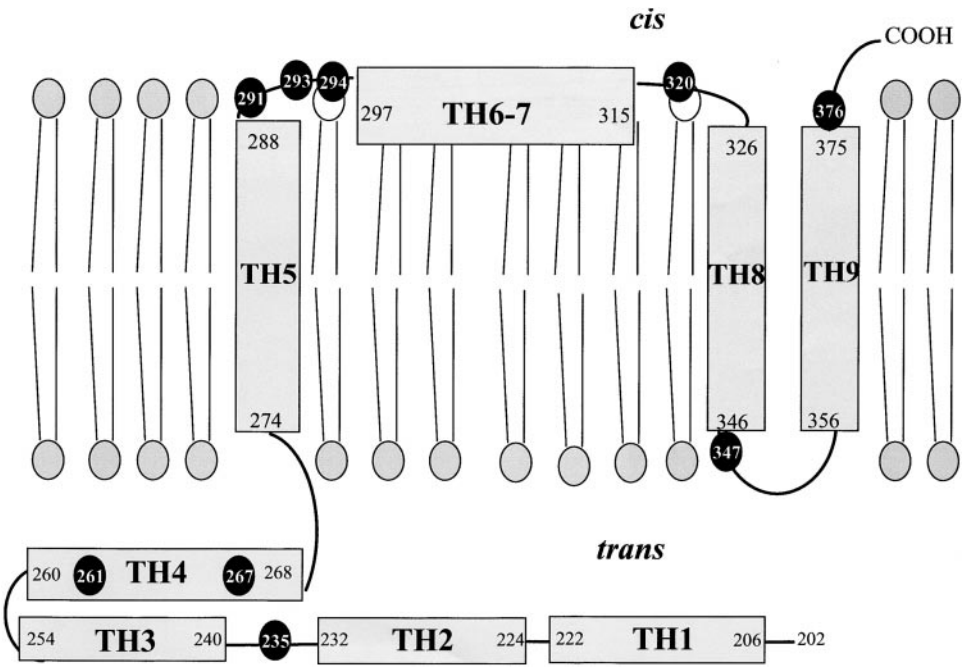

Figure 10. Our model of the distribution of T domain residues in the open channel state. Residues whose positions were determined in this study are shown in black with white numbers.

Validity of the H6 Tag and Biotinylation–Streptavidin Assays

A basic assumption in using these assays to determine T domain topography is that the H6-tagged and biotinylated sites end up on the same side of the membrane as where they normally reside when unencumbered by these labels. There are two reasons for believing this. First, the assays' results are consistent with previous findings. Their placement of residues 235, 261, and 267 on the trans side agrees with there being a site (or sites) between residues 209 and 265 susceptible to trans trypsin (Senzel et al., 1998). Similarly, the assignments of residues 320 and 376 to the cis side and residue 347 to the trans side are consistent with the previously determined membrane orientation of the TH8-9 region (Mindell et al., 1994a,b; Huynh et al., 1997).

Second, the assays were largely in agreement, even though the H6 tag is very hydrophilic and the biotin moiety (plus its linker) rather nonpolar. Only in the region of residues 291–299 is there a possible discrepancy. While residues 291, 293, and 294 appear cis by the H6 assay, the latter two, when biotinylated, do not induce normal channel formation. Furthermore, the cis streptavidin-induced increase in current noise for biotinylated 291 mutant was not reversible. Biotinylated 291

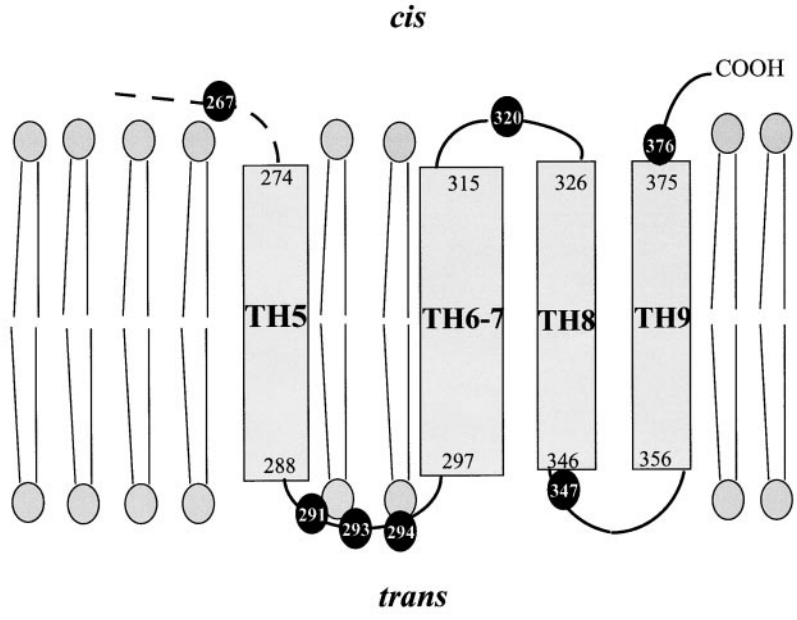

Figure 11. Double dagger model of Choe et al. (1992). See text for discussion of incompatibilities between this model and ours (Fig. 10).

mutant produced a much greater conductance (when cis pH was not raised) after cis TCEP addition, which suggests that biotinylation may decrease channel-forming efficiency. Thus, attaching biotin or H6 peptide may have held these residues on the cis side when they would otherwise have entered or traversed the membrane. However, biotin and H6 peptide did not prevent residues 235, 261, and 267 from traversing the membrane. Moreover, even if residues 291, 293, or 294 are indeed artificially held on the cis side by the H6 peptide, the amino terminus of the T domain is still translocated to the trans side. We showed this by attaching the H6 peptide at residue 293 with the amino-terminal H6 tag also present; the amino-terminal H6 tag closed the channels at negative voltages, while the attached H6 tag at residue 293 closed them at positive voltages (Fig. 12).

Should it turn out that residues 291, 293, and 294 were artifactually held on the cis side by the attached moieties and that they are normally on the trans side in the open channel state, the double dagger model in Fig. 11 is still precluded, because of our placement of residue 267 on the trans side. What we would have, instead of the disposition of residues shown in Fig. 10, is that, instead of TH5 being a membrane-spanning segment, TH6-7 would be membrane spanning, with everything upstream of it lying on the trans side.

The failure of the H6 tag at residue 347 to block the channel may result from its being in the channel-forming region; perhaps the H6 tag tethered there lacks the flexibility to reach its binding site with the correct orientation. Alternatively, the H6 tag attached at residue 347 may prevent channel formation, so that the observed conductance actually resulted from a minority of mutant 347 molecules that lacked the attached H6 tag because they failed to react with the maleimidyl-H6 peptide.

Certain aspects of the biotinylation–streptavidin results are puzzling. (a) As noted in results, the increased current noise produced by streptavidin's binding to biotinylated 235, 261, 267, 291, and 376 mutants is not reflected in increased single-channel current noise. It may result from a streptavidin-induced cooperative interaction among channels, but its nature and mechanism are unknown. (b) It is surprising that the biotin–streptavidin complex formed by trans streptavidin's binding to biotinylated 235, 261, and 267 mutants does not impede the amino-terminal H6 tag's access to the channel's binding site. (c) That trans streptavidin's binding to the biotinylated 347 mutant closes or blocks the channels is not surprising since that residue lies in the channel's ion-conducting pathway (Huynh et al., 1997), but why do ~20% of the channels remain unaffected? Conceivably, in a subpopulation of the channels, the tethered biotin is locked into a configuration inaccessible to trans streptavidin. (d) Occasionally, cis addition of biotinylated 235 mutant preincubated with streptavidin produced a large burst of conductance corresponding to very rapid insertion of hundreds of channels. Surprisingly, these channels displayed gating indicating that the amino terminus was translocated across the membrane, despite residue 235 being bound by streptavidin. Possibly, this rapid insertion of channels occurred through a transient membrane defect induced by their TH8-9 regions, which allowed the normally translocated region to cross the membrane with its attached streptavidin.

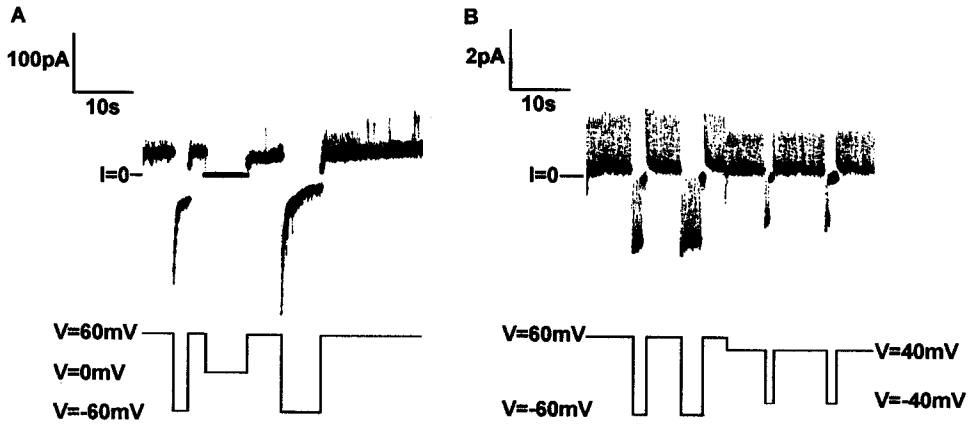

Figure 12. T domain channels having both an H6 peptide chemically linked at residue 293 and an amino-terminal H6 tag are blocked at positive voltages by the former and at negative voltages by the latter. Before the start of each record, T domain with H6 peptide attached at residue 293, as well as an amino-terminal H6 tag, was added to the cis compartment to a concentration of ~100 (A) or 1 (B) ng/ml. (A) After addition of T domain, conductance rose over time to the level seen at the start of the record, when the voltage was held at +60 mV. When the voltage was switched to −60 mV, the conductance was initially much larger, and then decreased rapidly to nearly zero. (This was consistent with initial unblocking by the H6 tag at residue 293, followed by amino-terminal H6 tag–mediated blocking.) When the voltage was switched back to +60 mV, the conductance was only a fraction of its expected value, namely the initial conductance at −60 mV before channel turn-off. (This was consistent with very fast blocking by H6 tag linked at residue 293.) (B) A single T domain channel flickered between the open state and a zero-conductance blocked state at +60 mV, spending most of its time in the zero-conductance state. When the voltage was switched to −60 mV, the channel became unblocked for a brief time, and then closed. When the voltage was switched back to +60 mV, the channel reopened immediately and resumed its flickering to the zero-conductance state. Similar behavior was seen at ±40 mV. Solutions and filtering were as given in Fig. 5.

Comparison of Planar Bilayer Results with Results in Other Systems

The T domain topography presented in Fig. 10 comes from the results described in this paper and is consistent with earlier cited results on planar lipid bilayers; it pertains exclusively to the open channel state. The topography of all, or parts, of the T domain has also been derived from fluorescence, spin-label, and protease–protection assays on lipid vesicles and cells. In the following brief summary of these results and their comparison to our planar bilayer findings, the reader should keep in mind that the number of open channels (a few thousand at most) in a given planar bilayer represents a minute fraction ($<10^{-10}$) of the total number of T domain molecules added to the cis compartment, and we know neither how many of these molecules are adsorbed onto the membrane surface, nor their membrane topography. In contrast, experiments on lipid vesicles and cell membranes generally measure the average disposition of all of the T domain molecules, of which an unknown and perhaps a very small fraction are in the open channel state.

The lipid vesicle conclusions agree with ours for the TH8-9 region; namely, it is inserted into the bilayer like a hairpin, with the residues near 349 close to or on the trans side, and residues near 320 and 376 close to or on the cis side (Oh et al., 1996; Quertenmont et al., 1996; Wang et al., 1997; Kachel et al., 1998). The cell data do not make as strong a statement about the orientation of the TH8-9 region, but they are consistent with the lipid vesicle and planar bilayer results in that this region is protected from cis protease digestion (Moskaug et al., 1991), and the mutation of either Glu349 or Asp352 to Lys inhibits toxicity and channel formation (Silverman et al., 1994b; Lanzrein et al., 1997).

Protease experiments on lipid vesicles do not agree with our proposed orientation of the TH5-7 region in Fig. 10. In vesicles, the entire TH5-7 region is completely digested by cis proteinase K (Quertenmont et al., 1996), whereas our model predicts that at least TH5 should be protected from digestion. Protease data on cells, however, are consistent with our orientation of the TH5-7 region, in that residue 299 is exposed on the cis side, whereas helices TH5 and TH6-7 are protected from digestion (Moskaug et al., 1991). The cell data are also consistent with our placing the loop connecting TH5 and TH6-7 on the cis side (rather than on the trans side as diagrammed in Fig. 11), in that mutating either Asp290 or Glu292 to Lys does not reduce toxicity or channel formation (Silverman et al., 1994b). [The mutation of Asp295 to Lys reduces toxicity and channel formation in cells (Falnes et al., 1992; Silverman et al., 1994b; Lanzrein et al., 1997), but given that the mutations to Lys of the nearby Asp290 or Glu292 do not, the effect of the Asp295-to-Lys mutation cannot be interpreted as simply resulting from placing a positive charge in the loop.]

Protease experiments on lipid vesicles agree marginally with our results for the region upstream of TH5. The amino terminal end of the T domain down to approximately residue 249 was protected from digestion by cis proteases, but this represented only 12% of the amount of TH8-9 protected (Quertenmont et al., 1996). We, on the other hand, place the amino-terminal end down to at least residue 267 on the trans side. Moreover, in the experiments by Quertenmont et al. (1996), the entire catalytic domain was digested by cis proteases, whereas in planar bilayers this is translocated to the trans side (Oh et al., 1999) and should therefore have been protected from digestion. In addition to the caveats mentioned at the beginning of this section, we also note that in these experiments the proteases were allowed to act for hours, making their correspondence to the planar bilayer experiments even more problematic. In cells, the amino-terminal end of the T domain was digested by pronase E (Moskaug et al., 1991), thereby placing this region on the cis side, in disagreement with our findings.

In sum, by picking and choosing, one can select data from vesicle and cell membrane experiments supporting most of the T domain topography proposed in Fig. 10. As noted at the start of this section, however, we feel it is a priori very difficult to relate the results of those experiments to ours of the open-channel state.

We thank Mike Rosconi and Dr. Erwin London for providing some T domain cysteine mutants, Dr. Karen Jakes for help with mutagenesis, and Drs. Paul Kienker and Karen Jakes for their helpful discussions.

This work was supported by National Institutes of Health grants T-32-GM07288 (L. Senzel), AI-22021 (R.J. Collier), and GM-29210 (A. Finkelstein).

Submitted: 15 December 1999
Revised: 7 February 2000
Accepted: 7 February 2000

REFERENCES

Bennett, M.J., S. Choe, and D. Eisenberg. 1994. Refined structure of dimeric diphtheria toxin at 2.0 Å resolution. *Prot. Sci.* 3:1444–1463.

Choe, S., M.J. Bennett, G. Fujii, P.M.G. Curmi, K.A. Kantardjieff, R.J. Collier, and D. Eisenberg. 1992. The crystal structure of diphtheria toxin. *Nature.* 357:216–222.

Donovan, J.J., M.I. Simon, R.K. Draper, and M. Montal. 1981. Diphtheria toxin forms transmembrane channels in planar lipid bilayers. *Proc. Natl. Acad. Sci. USA.* 78:172–176.

Draper, R.K., and M.I. Simon. 1980. The entry of diphtheria toxin into the mammalian cell cytoplasm: evidence for lysosomal involvement. *J.Cell Biol.* 87:849–854.

Eriksen, S., S. Olsnes, K. Sandvig, and O. Sand. 1994. Diphtheria toxin at low pH depolarizes the membrane, increases the membrane conductance and induces a new type of ion channel in Vero cells. *EMBO (Eur. Mol. Biol. Organ.) J.* 13:4433–4439.

Falnes, P.O., I.H. Madshus, K. Sandvig, and S. Olsnes. 1992. Replacement of negative by positive charges in the presumed membrane-inserted part of diphtheria toxin B fragment: effect on membrane translocation and on formation of channels. *J. Biol. Chem.* 267:12284–12290.

Greenfield, L., M.J. Bjorn, G. Horn, D. Fong, G.A. Buck, R.J. Collier, and D.A. Kaplan. 1983. Nucleotide sequence of the structural gene for diphtheria toxin carried by corynebacteriophage b. *Proc. Natl. Acad. Sci. USA.* 80:6853–6857.

Huynh, P., C. Cui, H. Zhan, K.J. Oh, R.J. Collier, and A. Finkelstein. 1997. Probing the structure of the diphtheria toxin channel: reactivity in planar lipid bilayer membranes of cysteine-substituted mutant channels with methanethiosulfonate derivatives. *J. Gen. Physiol.* 110:229–242.

Kachel, K., J. Ren, R.J. Collier, and E. London. 1998. Identifying transmembrane states and defining the membrane insertion boundaries of hydrophobic helices in membrane-inserted diphtheria toxin T domain. *J. Biol. Chem.* 273:22950–22956.

Kagan, B.L., A. Finkelstein, and M. Colombini. 1981. Diphtheria toxin fragment forms large pores in phospholipid bilayer membranes. *Proc. Natl. Acad. Sci. USA.* 78:4950–4954.

Lanzrein, M., P.O. Falnes, O. Sand, and S. Olsnes. 1997. Structure–function relationship of the ion channel formed by diphtheria toxin in Vero cell membranes. *J. Membr. Biol.* 156:141–148.

Madshus, I., and H. Stenmark. 1992. Entry of ADP-ribosylating toxins into cells. *Curr. Top. Microbiol. Immunol.* 175:1–26.

Mindell, J.A., J.A. Silverman, R.J. Collier, and A. Finkelstein. 1994a. Structure–function relationships in diphtheria toxin channels. II. A residue responsible for the channel's dependence on trans pH. *J. Membr. Biol.* 137:29–44.

Mindell, J.A., J.A. Silverman, R.J. Collier, and A. Finkelstein. 1994b. Structure–function relationships in diphtheria toxin channels: III. Residues which affect the cis pH dependence of channel conductance. *J. Membr. Biol.* 137:45–57.

Moskaug, J., H. Stenmark, and S. Olsnes. 1991. Insertion of diphtheria toxin B-fragment into the plasma membrane at low pH. *J. Biol. Chem.* 266:2652–2659.

Neilsen, O., and O. Buchardt. 1991. Facile synthesis of reagents containing a terminal maleimido ligand linked to an active ester. *Synthesis.* 10:819–821.

Oh, K.J., L. Senzel, R.J. Collier, and A. Finkelstein. 1999. Translocation of the catalytic domain of diphtheria toxin across planar phospholipid bilayers by its own T domain. *Proc. Natl. Acad. Sci. USA.* 96:8467–8470.

Oh, K.J., H. Zhan, C. Cui, K. Hideg, R.J. Collier, and W.L. Hubbell. 1996. Organization of diphtheria toxin T domain in bilayers: a site-directed spin labeling study. *Science.* 273:810–812.

Qiu, X.-Q., K.S. Jakes, A. Finkelstein, and S.L. Slatin. 1994. Site-specific biotinylation of colicin Ia: a probe for protein conformation in the membrane. *J. Biol. Chem.* 269:7483–7488.

Qiu, X.-Q., K.S. Jakes, P.K. Kienker, A. Finkelstein, and S.L. Slatin. 1996. Major transmembrane movement associated with colicin Ia channel gating. *J. Gen. Physiol.* 107:313–328.

Quertenmont, P., R. Wattiez, P. Falmagne, J.M. Ruysschaert, and V. Cabiaux. 1996. Topology of diphtheria toxin in lipid vesicle membranes: a proteolysis study. *Mol. Microbiol.* 21:1283–1296.

Sandvig, K., and S. Olsnes. 1980. Diphtheria toxin entry into cells is facilitated by low pH. *J. Cell Biol.* 87:828–832.

Senzel, L., P.D. Huynh, K.S. Jakes, R.J. Collier, and A. Finkelstein. 1998. The diphtheria toxin channel-forming T-domain translocates its own NH_2-terminal region across planar bilayers. *J. Gen. Physiol.* 112:317–324.

Silverman, J.A., J.A. Mindell, H. Zhan, A. Finkelstein, and R.J. Collier. 1994a. Structure–function relationships in diphtheria toxin channels: determining a minimal channel-forming domain. *J. Membr. Biol.* 137:17–28.

Silverman, J.A., J.A. Mindell, A. Finkelstein, W.H. Shen, and R.J. Collier. 1994b. Mutational analysis of the helical hairpin region of diphtheria toxin transmembrane domain. *J. Biol. Chem.* 269: 22524–22532.

Wang, Y., K. Kachel, L. Pablo, and E. London. 1997. Use of Trp mutations to evaluate the conformational behavior and membrane insertion of A and B chains in whole diphtheria toxin. *Biochemistry.* 36:16300–16308.

Zhan, H., K.J. Oh, Y.K. Shin, W.L. Hubbell, and R.J. Collier. 1995. Interaction of the isolated transmembrane domain of diphtheria toxin with membranes. *Biochemistry.* 34:4856–4863.